Estimation of x-ray parameters in digital coronary angiography for compensation of myocardial perfusion measurements

Corstiaan J. Storm[a], Cornelis H. Slump*[b]
[a]Dept. of Cardiology, Hospital Walcheren, Vlissingen, the Netherlands
[b]Dept. of Electrical Eng., University of Twente, Enschede, the Netherlands

ABSTRACT

Coronary angiography is the primary technique for diagnosing coronary abnormalities as it is able to locate precisely the coronary artery lesions. However, the clinical relevance of an appearing stenosis is not that easy to assess. In previous work we have analyzed the myocardial perfusion by comparing basal and hyperemic coronary flow. This comparison is the basis of a Relative Coronary Flow Reserve (RCFR) measure. In a Region-of-Interest (ROI) on the angiogram the contrast is measured as a function of time (the so-called time-density curve). The required hyperemic state of exercise is induced artificially by the injection of a vasodilator drug *e.g.* papaverine. In previous work we have presented the results of a small study of 20 patients. In this paper we present an analysis of the sensitivity of the method for variations in X-ray exposure between the two runs due to the Automatic Exposure Control (AEC) unit. The AEC is a system unit with the task to ensure a constant dose rate at the entrance of the detector by making the appropriate adaptations in X-ray factor settings for patients which range from slim to more obese. We have setup a phantom study to reveal the expected exposure variations. We present several of the developed phantoms together with a compensation strategy.

Keywords: Quantitative Coronary Angiography, perfusion myocardium, Computer Aided Diagnosis, Automatic Exposure Control

1. INTRODUCTION

Coronary angiography is still the major imaging technique to diagnose coronary abnormalities such as stenoses causing the clinical syndrome angina pectoris. In clinical cardiology the measure of a stenosis in a coronary artery is in standard practice still based on visual assessment leading to large inter and intra observer variability in reading coronary arteriograms.[1-3] Image analysis and computer assistance do result in a more consistent judgment, however, this approach is mainly based upon static geometric parameters such as percentage of diameter and area reduction of a single segment of the stenosed artery. [4-5]

In 70-90% of the coronary angiograms there are abnormalities to justify the diagnosis angina pectoris, however, in the 10-30% of the coronary angiograms there are no abnormalities at all in the epicardial vessels although the patients do have real anginal complaints.[6] This group of patients may benefit from additional diagnostic procedures demonstrating disturbances in the micro circulation of the myocardium.

The microcirculation of the myocardium is responsible for the functional capacity of the myocardial cells. The extent of myocardial perfusion to nourish the myocardial cells is regulated on demand and activated by local and general factors: exercise, stress and many others. The imbalance of demand and supply causes complaints such angina pectoris or heart failure.

The anatomical basis of the microcirculation consists of a proximal and distal compartment in which the prearterioles in the proximal compartment regulate the perfusion pressure in the arterioles. The arterioles are sparsely innervated resulting in a regulation mostly depended on local factors in particular the oxygen concentration.

*c.h.slump@ewi.utwente.nl; phone (+31) 53 4892094; fax (+31) 53 4891060; www.sas.el.utwente.nl

Through this mechanism the coronary flow is regulated in proportion to the need of the myocardium for oxygen, which is closely related to the amount of cardiac work load. In the absence of disease in the epicardial vessels there is hardly any resistance to the flow in these vessels in contrast to the micro vascular component. So the microvascular vessels determine the amount of blood the myocardium will get in a factor three to six times the basal amount depending on the demand. This is called Coronary Flow Reserve (CFR).[7-8] Coronary flow reserve depends mostly on the dilation of the arterioles.

If multi angulated angiograms have reduced the likelihood of the presence of asymmetric lesions, other diagnostic tests become necessary. In that case micro vascular dysfunction can be excluded by measuring coronary flow reserve. The CFR is measured by pharmacologic intervention to get maximal vasodilatation, *i.e.* papaverine.

There are several methods to measure the CFR: invasively or non-invasively. The non-invasive methods are using radioactive materials (nuclear medicine), the invasive technique consist of mostly expensive catheters for measuring flow differences in the epicardial vessels in basal conditions and after pharmacologic interventions. In[9] we have described a method based upon standard angiographic image sequences to evaluate the extent of possible dilatation of the arterioles after pharmacologic intervention in an easy way without extra catheters or procedures in connection of a normal coronary angiography using the standard. Basically the basal and hyperemic states are compared by the slope of the time-density curve, leading to the Relative Coronary Flow Reserve (RCFR).[8] In[9] we have described the results of a small clinical study with 20 patient cases. In the present paper we investigate the sensitivity of the method for exposure variations induced by the Automatic Exposure Control (AEC) unit of the diagnostic imaging X-ray system. This paper is organized as follows. In the next section we describe a phantom experiment mimicking the myocard perfusion in order to obtain the ramp response of the AEC unit. A few other phantom experiments are also described in somewhat more detail and the experiments lead to a hypothesis about the working of the AEC unit. This hypothesis is further evaluated and results are presented of a compensation method of exposure variations. We finalize with a discussion and conclusions.

2. METHODS

2.1 RCFR model

The relation between coronary pressure and flow has been studied by many authors and has resulted in a variety of models[10] with varying complexity. Basic element in many models is that the vasodilation of the arterioles regulates the flow through the myocard. A stenosis influences the flow only if its resistance is of the same order of magnitude as the resistance by the myocard, *i.e.* as the arterioles are totally dilated. This insight has stimulated the search for a physiologic measure of the severity of a stenosis[11].

With CFR the measured local maximum contrast density represents the vascular volume and the measured local contrast arrival time is taken to be inversely proportional to flow[12]. In a Region-of-Interest (ROI) on the angiogram (without an overlaying major blood vessel) the contrast is measured as a function of time (the so-called time-density curve). The required hyperemic state of exercise can be induced artificially by the intracoronary injection of a vasodilator drug *e.g.* papaverine. In this hyperemic state, in contrast to the basal state, the arterioles are maximally dilated, thus the normally increasing the blood flow to the physical limits is set by the sizes of the epicardial coronary arteries and especially the stenosed segments. Although good results with the CFR method have been reported[13-15], in clinical practice the procedure is demanding, especially the correction of the background contributions is difficult because of the contracting heart dynamics. The requirement is that the two image sequences, basal and hyperemic, should be registered exactly the same. However, movements due to patient respiration cannot be eliminated completely. In order to avoid misregistration artifacts, pacing of the heart together with ECG triggered contrast injection and image acquisition appeared to be mandatory.

As the measurement of the absolute CFR is difficult[16], alternatives such as the Relative Coronary Flow Reserve (RCFR)[8] and the Fractional Flow Reserve (FFR)[17] have been developed. Dual energy subtraction[18] has been proposed to overcome the motion artifacts.

In a simple model of the integration over a ROI positioned on the myocard in the angiogram, we assume that within the ROI there are no overlaying major arteries. The integration *i.e.* the summation of the (log of the) pixel intensities inside the ROI together with the radiographic projection basis of the angiogram, provides for a 3D volume measurement of the

amount of contrast agent contained in the myocard. We assume that the injected contrast completely replaces the blood. The myocard can be considered to be a reservoir which holds temporarily the contrast agent for a certain mean transit time τ_{transit}. The result of the integration is proportional to the concentration contrast material under the ROI. A schematic diagram of the myocard model is shown in figure 1, the inflow of contrast at the arterial side is $I(t)$, the outflow is at the venous side.
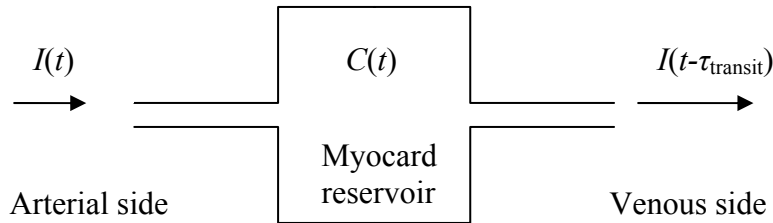

Fig.1 Schematic diagram of the ROI integration resulting in the contrast concentration $C(t)$ in the myocard reservoir.

The single pass output of the integration over the reservoir with mean transit time τ_{transit} is given by the contrast concentration $C(t)$:

$$C(t) = \begin{cases} 0, & t < \tau_{inject} \\ \int_{\tau_{inject}}^{t} I(\tau)d\tau, & \tau_{inject} < t < \tau_{peak} \\ C_{\max}, & \tau_{peak} < t < \tau_{transit} \end{cases} \tag{1}$$

After a certain time τ_{peak} the contrast concentration saturates as the whole contrast bolus is contained in the myocard. The contrast concentration starts to diminish after the mean transit time τ_{transit}. The contrast concentration is shown in figure 2.
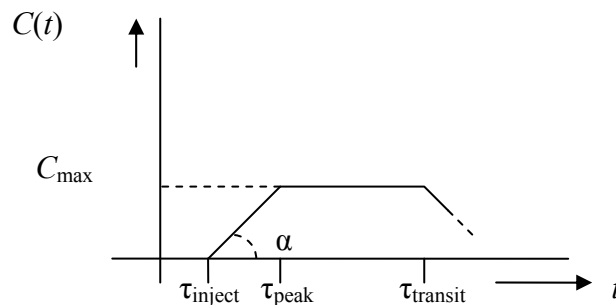

Figure 2 The contrast concentration $C(t)$ and the describing parameters. Of special interest is the slope α as it is related to the flow.

The rising slope of the *C(t)* curve of figure 2 is proportional to flow. Our method compares this slope in basal and hyperemic conditions. There is a small time - offset between the moment of injection and the start of the image sequence. In the ECG guided selection we take our first image slightly before the second R – peak after the start of the run.

2.2 Phantom study

We have developed several static and dynamical phantoms to study the response of the imaging system under control of the AEC unit for the cardiac acquisition protocols installed in the system. In all cases we have 20 cm of water mimicking the patient in order to ensure a normal clinical imaging condition. The static phantoms consist of extra attenuating material, e.g. different steps of perspex and aluminum which are placed at different locations in the imaging field. The resulting images show the response of the AEC on the different positions of the extra absorbing material. With the dynamic phantoms we measure the time response of the AEC. We present a slowly in time increasing or deceasing amount of water to the imaging system and from this ramp-response in theory one should be able to obtain the step response in time.
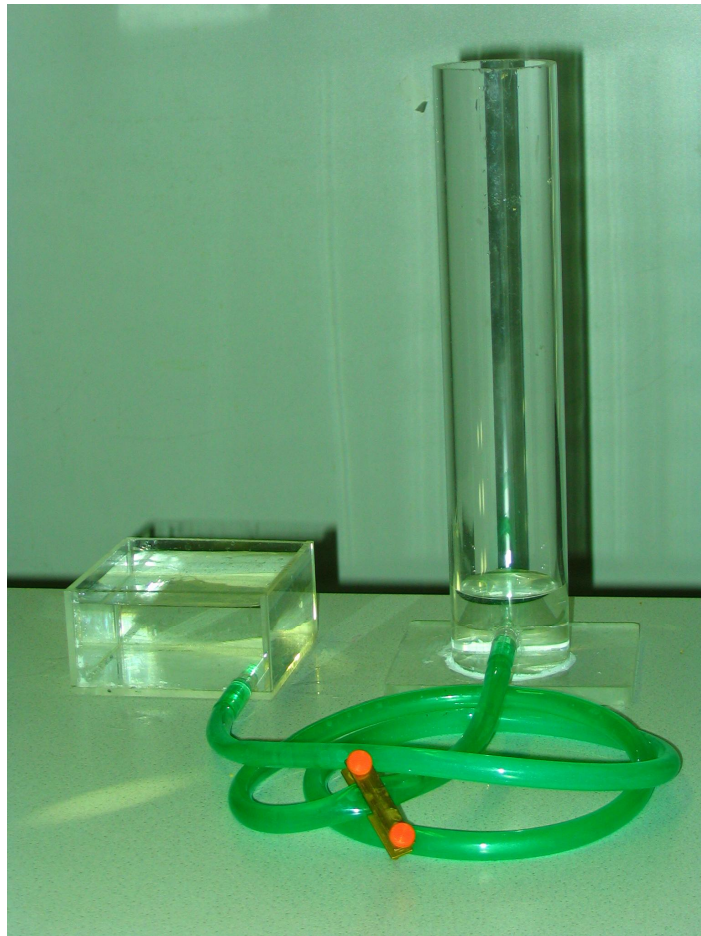

Fig. 3 A small Perspex bucket of length × breadth × height of 10 cm × 10 cm × 5 cm. The thickness of the Perspex is 4 mm. The speed of water inflow or outflow can be simply adjusted.

3. DATA ANALYSIS

The images analyzed in this paper are acquired with an Axiom Artis dFC single plane C-arm system with a dynamic flat detector for cardiology from Siemens Medical Solutions. The frame rate is 15 frames / second. In clinical runs, the ECG is recorded simultaneously during acquisition. In figure 4 an acquired image in anterior posterior projection is shown of the water phantom depicted in figure 3, together with the selected ROI used for intensity integration. The bucket was filled to a height of 4 cm with water. The bucket was depleted in 10 s meanwhile 151 images have been acquired. Following our procedure for the computation of the RCFR we integrate the image intensity over the square ROI positioned just inside the bucket. The integrated pixel intensity over the ROI is shown in figure 5.

a   b
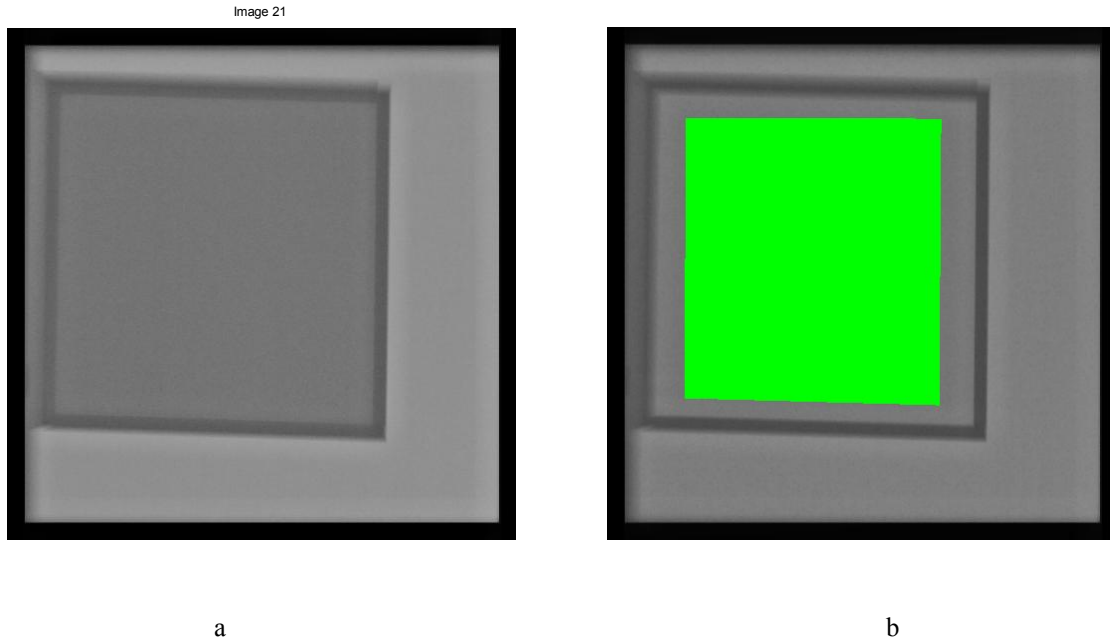
Figure 4 X-ray projection image of the water phantom of figure 3 (a) and the selected ROI for intensity integration (b).
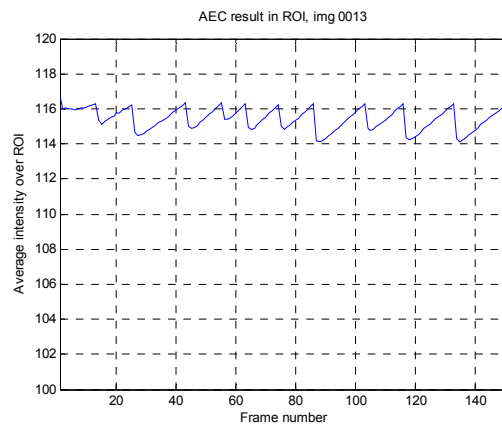

Figure 5 Average pixel intensity over the ROI indicated in figure 4, showing the effect of the water depletion.

A similar average pixel intensity profile over consecutive frames is obtained if we increase the water level from 0 to 4 cm in several seconds of time. In order for our RCFR method to be valid we have to obtain intensity profiles as depicted in figure 2 with up and down slopes proportional to the filling / depletion rate. On the contrary we observe almost constant intensity. Apparently the AEC controls the intensity with a certain margin around the pixel value 115. The AEC counter acts the dynamic effects we want to observe. Therefore we look into more detail into the behavior of this system unit. In the documentation of the vendor the required information could not be found. In the pre-digital analog film era, in general the task of the AEC was to ensure an average film density D in a central area of the film recording of the image. Often $D \cong 1$ was chosen, for this is for the most films a point on the H-D curve with the steepest slope which means a good contrast while maintaining the excellent dynamic range of film.

With digital processing techniques abundantly available and in combination with the digital X-ray detector a far more complicated AEC can be thought of. One can think of intelligent ways to optimize image contrast, minimizing X-ray dose and required amount of iodine to be injected, kVp selection, tube power control, multiple measuring fields adaptive to the patients anatomy, and so on.

We have performed the following experiment to analyze the behavior of the AEC unit. We acquire images of a uniform object of 20 cm water while we close the left and right hand X-ray shutters. In a new run we open the shutters again. In the closing we observe that the image intensity is fairly constant until the shutters have come in more than just half way. For the shutter opening run, we obtain a constant intensity after half way opening. In order to visualize the AEC response, we average the rows of each consecutive image and synthesize a new image. These are displayed in figure 6 and 7, respectively.
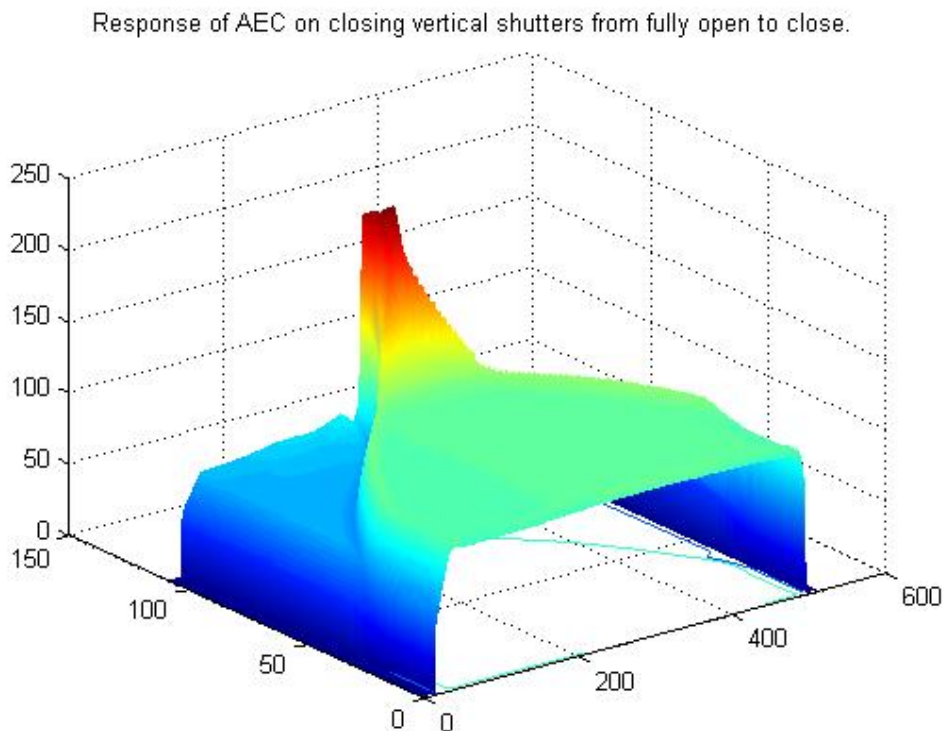

Fig. 6 The row averaged image sequence of a closing of the left and right hand shutters shows an almost constant level until about half closure.

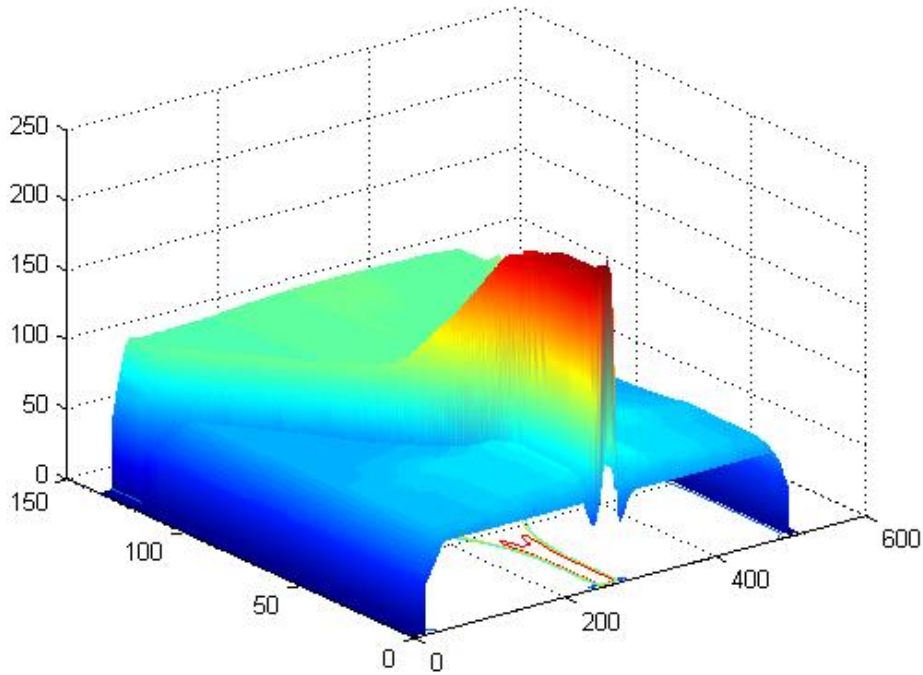Response of AEC on opening vertical shutters from closed to fully open.

Fig. 7. The row averaged image sequence of an opening of the left and right hand shutters shows an almost constant level after about half way.

First we have simulated the AEC behavior with square measuring fields in order to reproduce the AEC behavior as revealed in figures 6 and 7. Square measuring fields are easy to evaluate in real-time enabling update of the exposure parameters on a frame – to – frame basis. After ample simulation experiments, however, we hypothesize a circular AEC measuring field of 50% diameter central in the image with as control set point an average value. In order to test this hypothesis we analyze the average pixel intensity in this central and circular 50% diameter measuring field for a clinical basal case. In figure 8 we present the AEC measuring field for an image of the clinical sequence.
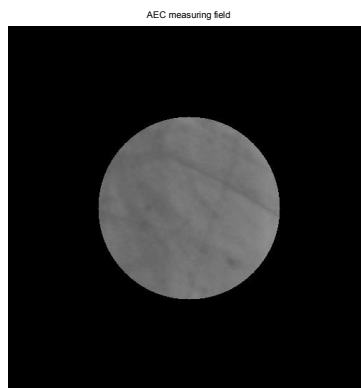

AEC measuring field

Fig. 8 The hypothesized AEC measuring window is here shown for a clinical case depicting a part of the myocard.

Figure 9 shows the obtained average pixel intensity over the AEC window. The clearly observable regular intensity variations match very well with the patient's ECG signal corresponding to this run.
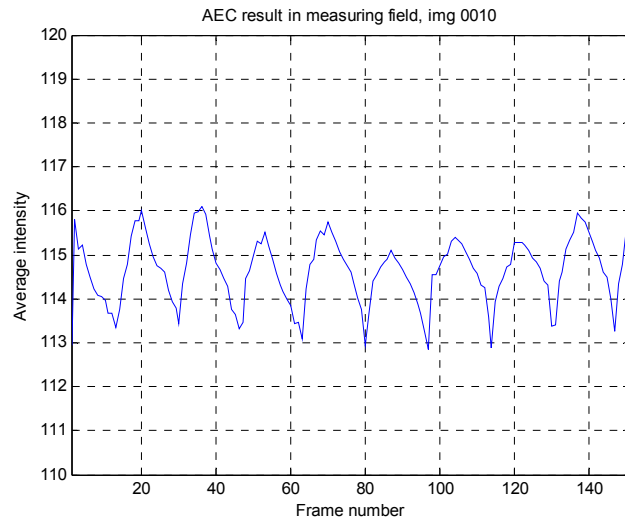

Fig. 9 Average pixel intensity over the AEC window indicated in figure 8 of a clinical case, showing intensity variations than can be related to the patient's ECG.
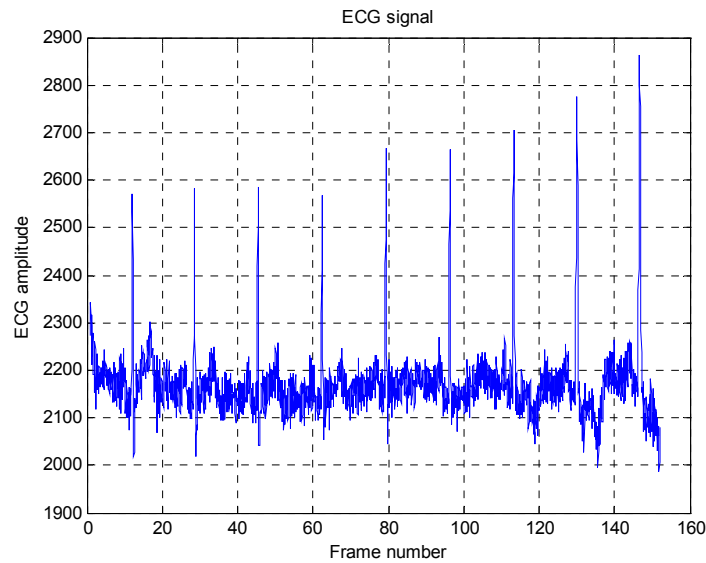

Fig. 10 Patient ECG signals corresponding to the clinical image sequence of figure 9.

If we compare the location of the valleys in figure 9 with the R-peaks in the ECG in figure 10, we have a good correspondence. At the R-peak the heart is maximally filled with blood and the contraction starts which correspond with the highest X-ray absorption and thus minimal image intensity. These findings give us confidence about the AEC window and average value set point control.

We now return to our bucket of water experiment and set our goal to use our obtained knowledge to compensate for the AEC response on the water level changes. Our aim is to obtain intensity profiles similar to figure 2. We therefore apply a

second measuring ROI outside the projected water bucket and outside the AEC measuring window. Figure 11 shows the two ROI's that we apply.

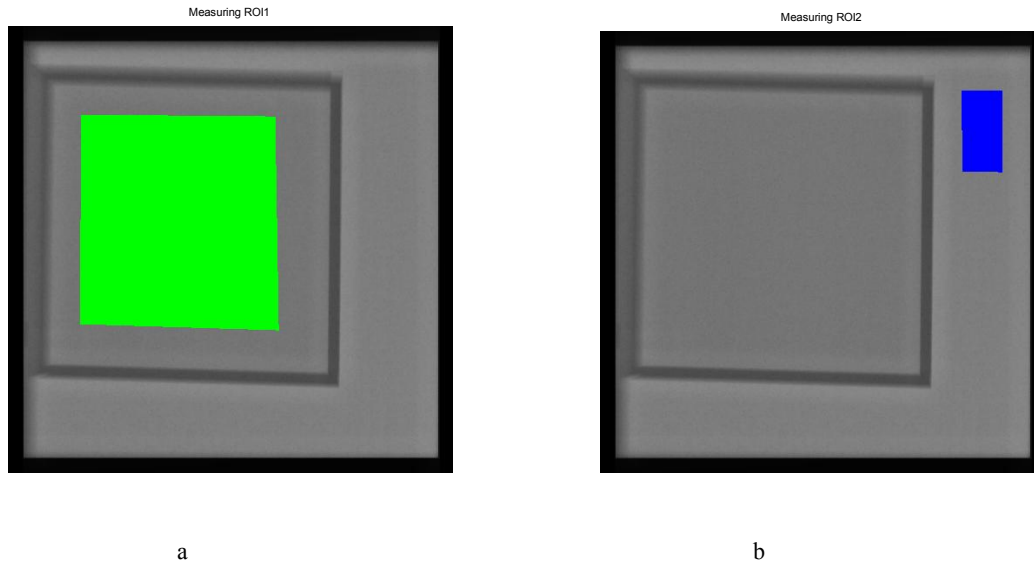a   b

Fig. 11 The position and size of ROI1 inside the bucket projection is shown in green (a) and the position and size of ROI2 in blue of which the purpose is to measure the AEC response (b).

The obtained integrated pixel values over the ROI's are shown in figure 12. The result of ROI2 reveals the response of
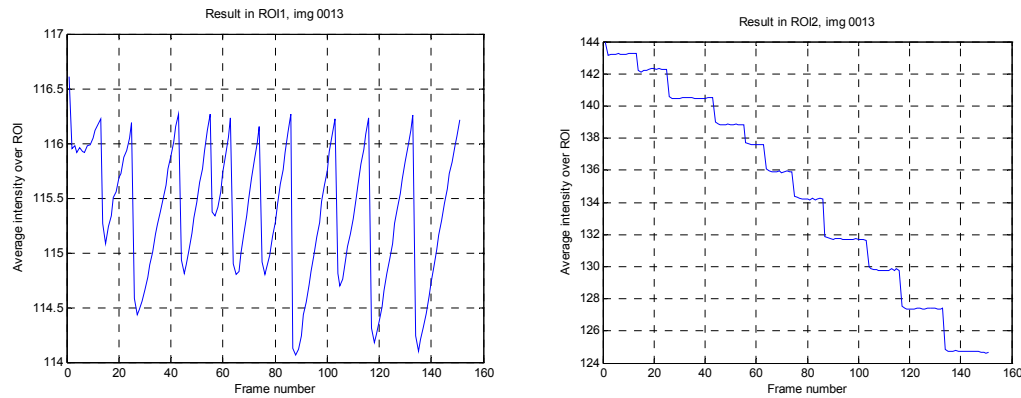

Fig. 12 Obtained integrated results corresponding to ROI1 (left) and ROI2 (right) of figure 11.

AEC to the slowly decreasing water height. The discontinuities in both curves of figure 12 do match each other. The curves can be combined and from that we can normalize the ROI integration over the water bucket proportional to the water height. This is precisely what we need for the RCFR method. Ironically, with measuring outside the ROI of the water bucket we obtain the result of the changing water height inside. The procedure works also fine for increasing water levels as is shown in figure 13 (with similar ROI positions as in figure 11.) The depletion of the bucket is much smoother than the filling. The graphs reflect the filling vertices.

Result in ROI1, img 0014
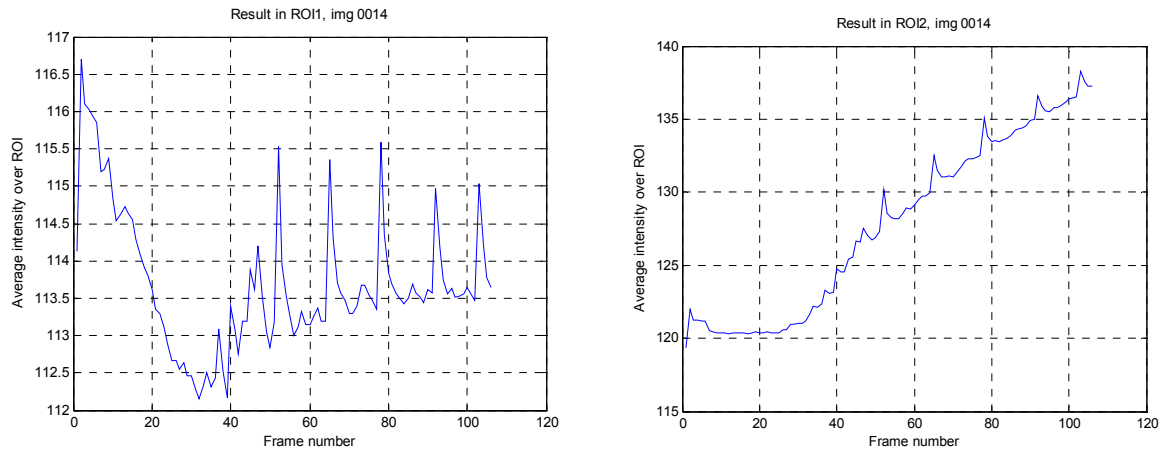
Result in ROI2, img 0014

Fig. 13 Obtained integrated results corresponding to ROI1 (left) and ROI2 (right) similar to figure 11, now for the case of the filling of the bucket.

4. RESULTS

We have presented results of dynamic phantom studies. For the RCFR method it appeared to be necessary to take the AEC unit into consideration. The functioning of this device has been assessed with measurements and simulations leading to a verified function hypothesis. Based upon the function hypothesis, an intensity measurement ROI method has been implemented for the compensation of exposure intensity variations. The estimated compensated intensity profiles correspond with flow rates in the filling or depleting the bucket.

5. DISCUSSION AND CONCLUSIONS

Our long-term purpose is in the automated evaluation of the patho-physiological relevance of lesions, in the coronary arteries as revealed by angiography. We aim to extract as much as possible quantitative information about the physiological condition of the heart from standard angiographic image sequences. Coronary angiography is still the gold standard for evaluating and diagnosing Coronary Artery Disease (CAD) as it is able to precisely locate lesions and the length of it in the coronary artery imaged. The dimensions of the stenosis can be assessed nowadays successfully with image processing based Quantitative Coronary Angiography (QCA) techniques. This technique reveals only the (projected) shape of the lesion, but there is no information about the clinical, pathophysiological consequences of the stenosis. Our aim is to assess the clinical significance of the stenosis. In previous work[9] we have analyzed the myocardial perfusion as revealed in standard angiographic image sequences. Time - density curves are obtained over the myocardium separated from the overlaying coronary vessels. The slopes of these curves are proportional to flow and provide therefore the basis for the RCFR.

In this paper we show that the results of plain RCFR depend to a major extend on the X-ray exposure control dynamics, *i.e.* we want to measure the response of the vascular bed in the myocardium and not the response of the X-ray exposure control. Preferably we acquire the images with a fixed kVp and mAs during the acquisition of the image sequence. This option is, however, not provided by the vendor. In order to keep the protocol standard we therefore have to rely to compensation techniques.

We present the estimation of the image intensity response of the AEC by measuring over a ROI outside the AEC window and the results of the exposure intensity compensation which leads to a satisfactory result for our phantom study. The consequence on clinical cases has to be investigated further. Because the iodine contrast is sensitive to kVp shifts, we expect to need additional assessment with this respect.

REFERENCES

1. K.M. Detre, E. Wright, M.L. Murphy, T. Takaro, "Observer agreement in evaluating coronary angiograms," *Circulation* 52(6), 979-986 (1975).

2. L.M. Zir, S.W. Miller, R.E. Dinsmore, J.P. Gilbert, J.W. Hawthorne, "Interobserver variability in coronary angiography," *Circulation* 53(4), 627-632 (1976).

3. E.J. Topol, S.E. Nissen, "Our preoccupation with coronary luminology," *Circulation* 92(8), 23333-2342 (1995).

4. J.H.C. Reiber, P.W. Serruys, C.J. Kooijman, W. Wijns, C.J. Slager, J.J. Gerbrands, J.C.H. Schuurbiers, A. den Boer, P.G. Hugenholtz, " Assessment of short-, medium-, and long-term variations in arterial dimensions from computer-assisted quantitation of coronary cineangiograms," *Circulation* 71(2), 280-288 (1985).

5. J.H.C. Reiber, P.W. Serruys, *Quantitative Coronary Arteriography*, Kluwer Academic Publishers, 1991.

6. R.O. Cannon, P.G. Camici, S.E. Epstein,"Pathophysiological dilemma of syndrome X," Circulation 85(3), 883-892 (1992).

7. R.L. Kirkeeide, K.L. Gould, L. Parsel, "Assessment of coronary stenoses by myocardial perfusion imaging during pharmacologic coronary vasodilation. VII. Validation of coronary flow reserve as a single integrated functional measure of stenosis severity reflecting all its geometric dimensions," *J. Am. Coll. Cardiol*. 7(1), 103-113 (1986).

8. K.L. Gould, R.L. Kirkeeide, M. Buchi, "Coronary flow reserve as a physiologic measure of stenosis severity," J. Am. Coll. Cardiol. 15(2), 459-474 (1990).

9. C.J. Storm, C.H. Slump, "CAD of myocardial perfusion," Proceedings SPIE Medical Imaging, 6514, 20-22 Feb. 2007, San Diego CA.

10. F.J. Klocke, R.E. Mates, J.M. Canty, A.K. Ellis, "Coronary pressure-flow relationships, controversial issues and probable implications," *Circ. Res.* 56(3), 310-323 (1985).

11. K.L. Gould, K. Lipscomb, "Effects of coronary stenoses on coronary flow reserve and resistance," *Am. J. Cardiol.* 34, 48-55 (1974).

12. J.T. Cusma, E.J. Toggart, J.D. Folts, W.W. Peppler, N.J. Hangiandreou, C.S. Lee, C.A. Mistretta, "Digital subtraction angiographic imaging of coronary floe reserve," *Circulation* 75(2), 461-472 (1987).

13. R.A. Vogel, "The radiologic assessment of coronary blood flow parameters," *Circulation* 72(3), 460-465 (1985).

14. V. Legrand, G.B. Mancini, e.r. Bates, J.M. Hodgson, M.D. Gross, R.A. Vogel, "Comparative study of coronary flow reserve, coronary anatomy and results of radionuclide exercise tests in patients with coronary artery disease," *J.Am. Coll. Cardiol.* 8(5), 1022-1032 (1986).

15. G.B. Mancini, S.B. Simon, M.J. McGillem, M.T. LeFree, H.Z. Friedman, R.A. Vogel, " Automated quantitative coronary arteriography: morphologic and physiologic validation in vivo of a rapid angiographic method," *Circulation* 75(2), 452-460 (1987).

16. M.J. Kern, A. Lerman, J.-W. Bech, B. de Bruyne, E. Eeckhout, W.F. Fearon, S.T. Higano, M.J. Lim, M. Meuwissen, J.J. Piek, N.H.J. Pijls, M. Siebes, J.A.E. Spaan, "Physiological assessment of coronary artery disease in the cardiac catheterization laboratory: a scientific statement from the American heart association committee on diagnostic and interventional cardiac catheterization, council on clinical cardiology," *Circulation* 114(12), 1321-1341 (2006).

17. N.H.J. Pijls, B. van Gelder, P. van der Voort, K. Peels, F.A.L.E. Bracke, H.J.R.M. Bonnier, M.I.H. El Gamal, "Fractional flow reserve: a useful index to evaluate the influence of an epicardial coronary stenosis on myocardial blood flow," *Circulation* 92(11), 3182-3193 (1995).

18. S. Molloi, A. Ersahin, J. Tang, J. Hicks, C.Y. Leung, "Quantification of volumetric coronary blood flow with dual energy subtraction angiography," *Circulation* 93(10), 1919-1927 (1996).